(23) Miller, R. E.; Stein, S. E. *Prepr. Pap.-Am. Chem. Soc., Div. Fuel Chem.* **1979**, *24*, 271.
(24) Panvelker, S. V.; Shah, Y. T.; Cronauer, D. C. *Ind. Eng. Chem. Fundam.* **1982**, *21*, 236.
(25) Petrocelli, F. P. M.Ch.E. Thesis, University of Delaware, in preparation.
(26) Petrocelli, F. P.; Klein, M. T. "Simulation of Kraft Lignin Pyrolysis"; Proceedings, Fundamentals of Thermochemical Biomass Conversion: An International Conference, Estes Park, CO, 1982 (accepted).
(27) Poutsma, M. L. *Fuel* **1980**, *59*, 335.
(28) Sato, Y.; Yamakawa, T.; Onishi, R.; Kameyama, H.; Amano, A. *J. Jpn. Pet. Inst.* **1978**, *21*, 114.
(29) Sweeting, J. W.; Wilshire, J. F. K. *Aust. J. Chem.* **1962**, *15*, 89.
(30) Taylor, T. W. T.; Murray, A. R. *J. Chem. Soc.* **1938**, 2078.
(31) Vernon, L. W. *Fuel* **1980**, *59*, 102.
(32) Virk, P. S. *Fuel* **1979**, *58*, 149.
(33) Woodward, R. B.; Hoffmann, R. "The Conservation of Orbital Symmetry"; Verlag Chemie: Weinheim, 1970.

Molecular Modeling of Polymer–Dye Complexes Involving Homopolymers of Poly(*N*-vinylimidazole) and Methyl Orange

B. J. Orchard

Department of Macromolecular Science, Case Western Reserve University, Cleveland, Ohio 44106

J. S. Tan

Research Laboratories, Eastman Kodak Company, Rochester, New York 14650

A. J. Hopfinger*

Department of Macromolecular Science, Case Western Reserve University, Cleveland, Ohio 44106. *Received March 14, 1983*

ABSTRACT: Molecular modeling was used to study the intramolecular conformational behavior of neutral and fully quaternized poly(*N*-vinylimidazole) and the anionic form of methyl orange. Subsequently, intermolecular modeling of polymer–dye interactions was performed on the basis of the intramolecular findings. The purpose of the intermolecular studies was to identify a molecular geometry of the polymer–dye complex whose thermodynamic properties are consistent with experimental observations. This was achieved by assuming an isotactic chain segment of the polymer in a 3/1 helical conformation and an effective dielectric constant (in the Coulomb atom-pair potential) of 30. The polymer–dye binding complex is characterized by partial insertion (intercalation) of a phenyl ring of the dye between spatially adjacent polymer side-chain rings with the sulfonate of the dye located as close as possible to the charged imidazole nitrogen of the polymer.

Introduction

Tan and Handel[1] have investigated the binding behavior of methyl orange to homopolymers and copolymers of quaternized poly(*N*-vinylimidazoles) (PVI) in the presence of various counterions. The principal findings from these studies are as follows: (1) The apparent polymer–dye binding constant, log K_{app}, increases as the extent of binding, r, increases. (2) K_{app} for a given r and added salt decreases with an increase in ionic strength. The stoichiometry of the site–dye complex approaches unity as the polymer solution is saturated with excess dye. Stoichiometric unity is not realized for uncharged polymers. (3) The binding strength (or $-G$) at a given r decreases in the following order: BPVI (benzyl chloride quaternized PVI) > MPVI (methyl bromide quaternized PVI) > PVI. (4) The dye binding to MPVI and BPVI is identical in MeOH and is much weaker than in aqueous media. (5) The enthalpy of binding ($\Delta H°$) is exothermic and independent of ionic strength and/or type of counterion present in solution. (6) The $-\Delta H°$ of binding at low saturation (r = 0.01) decreases in the following order: BPVI > PVI > MPVI.

Some conclusions and an interpretation of the binding behavior can be summarized as follows: (1) Electrostatic and steric (van der Waals) interactions act jointly in controlling polymer–dye binding. The stoichiometry of the polymer–dye complex is governed by electrostatics (charge). (2) There is a direct competition between the dye and the counterions for polymer binding sites. (3) The electrostatic interactions have a net effect on the entropic contribution to binding and a lesser extent on the enthalpy. The measured $-\Delta H°$ of binding arises from polymer–dye (electrostatic and van der Waals) and dye–dye interactions (van der Waals). (4) An effective molecular "dielectric constant" of ~30 can be used to explain the observed thermodynamic properties when charge–charge interactions are modeled by a simple Coulombic function. (5) There is cooperative bound dye–dye interaction as opposed to independent-site binding. The degree of cooperativity decreases as the binding approaches saturation.

The goal of the work reported here has been to identify intermolecular charged polymer–dye molecular structures that are energetically stable and consistent with the observations and conclusions described above. A necessary corollary to this work has been an analysis of the molecular energetics, especially factors affecting electrostatic interactions. Molecular modeling has been carried out within the fixed-valence geometry molecular-mechanics formalism[2] for charged polymer segments and/or the dyes. The CHEMLAB molecular modeling laboratory[3] was used to perform the computational chemistry.

An important consideration, and likely limitation, of the results reported in this paper involves polymer tacticity. The experimental studies have used atactic polymer samples. It is not possible to explicitly model atactic structures in conformational structure calculations, owing to the random stereochemical behavior. We have considered only chain segments of all-isotactic and all-syndiotactic struc-

* Alternative address: Department of Medicinal Chemistry, Searle Research and Development, 4901 Searle Parkway, Skokie, IL 60077.

0024-9297/84/2217-0169$01.50/0

tures. Only the isotactic structure yields polymer–dye molecular geometries consistent with experimental observations and also stable according to the energy calculations.

Methods

Calculation of Intramolecular Energy. The total energy is partitioned into additive steric repulsive–dispersive, electrostatic, hydrogen-bonding, and torsional components. For simplicity, electrostatic and hydrogen-bonding energies have been grouped together and referred to as the electrostatic component throughout this paper. Steric interactions are represented by a set of Lennard-Jones 6–12 functions. The electrostatic interactions are modelled by a Coulomb potential function of the form

$$\phi_e(r) = \frac{Kq_iq_j}{\epsilon r_{ij}} \quad \text{(electrostatic)} \tag{1a}$$

$$\phi_h(r) = \left[\frac{a_{ij}}{r_{ij}^6} + \frac{b_{ij}}{r_{ij}^{12}}\right] \cos^4 2\theta_d \cos 3\theta_a + \frac{Kq_iq_j}{\epsilon r_{ij}}$$

(hydrogen bond) (1b)

The a_{ij} and b_{ij} terms redefine the Lennard-Jones 6–12 potential to account for the radial behavior of hydrogen bonding; θ_d and θ_a define the energy dependence of hydrogen bonding on donor and acceptor angular geometry.[2]

The Hopfinger[2] steric parameters have been used. The polymer backbone C–C torsional term is represented by a threefold potential function with a barrier height equal to 2.8 kcal/mol, and the C–I (I = imidazole ring) bond rotation has been modelled by a symmetric sixfold function having a barrier of 0.28 kcal/mol. The nonbonded interactions have been weighted/counted to model a chain of infinite length by the polymer-reduced interaction matrix method (PRIMM).[4] The equivalence rule has been assumed so that two rotational degrees of freedom are allowed along the polymer backbone. The interactions between and among backbone methylenes and CH–I–R groups up through six nearest-neighbor contributions have been considered in order to include the major interactions that contribute to conformational states up through 3/1 helices. R is either CH_3 or CH_2Ph for the methyl- or benzyl-quaternized poly(*N*-vinylimidazole), respectively.

The reference polymer conformation corresponds to the polymer backbone in an all-trans orientation. The imidazole ring is perpendicular to the polymer chain axis. If atoms $i, i+1, i+2, \ldots$ form the backbone, then the bonds are rotated by sighting along the bond i–$i+1$–$i+2, \ldots$ and rotating clockwise for positive values.

Calculation of Intermolecular Energy. Three different types of intermolecular interactions have been examined: (1) dye–dye, (2) dye–polymer, and (3) dye–(polymer–dye complex). The assumption has been made that each of the interacting components is rigid in conformation. Each molecule has been assigned its global (lowest) intramolecular energy conformational state. One molecule (always the polymer segment if it is being studied) has been fixed in space, and the other molecule is mobile. There are six spatial degrees of freedom for a binary intermolecular system (see Figure 1). The variables α, β, and γ refer to the rotation about the center of mass of the mobile molecule in an arbitrary internal coordinate frame; θ, d, and z are the cylindrical coordinates, that relate the position of the center of mass of the mobile molecule to an origin associated with the fixed molecule.

The intermolecular energy is the sum of the steric, electrostatic, and hydrogen-bonding interactions. Four different "molecular dielectric" values (3.5, 7.0, 30, and 60) have been considered. Variation of the dielectric factor permits an analysis of the role of this ill-defined property upon molecular energetics and geometry. The dielectric factor has been varied in this study even though experimental results[1] suggest that the effective molecular dielectric constant is about 30.

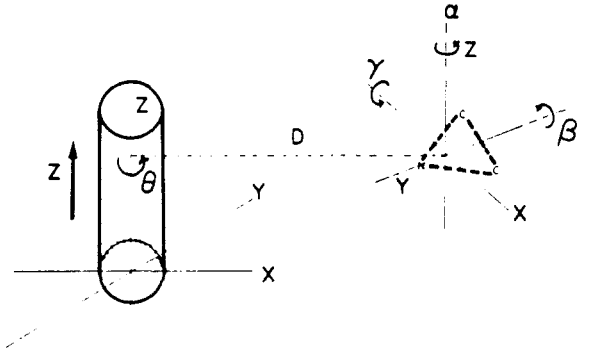

Figure 1. Intermolecular geometry and spatial variables to describe polymer–dye interactions.

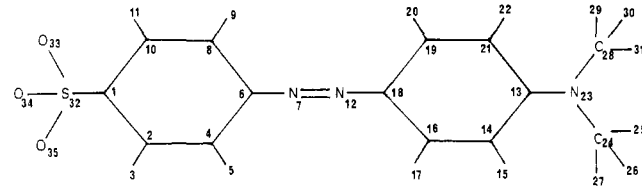

Figure 2. Atomic numbering schemes for methyl orange.

Table I
Valence Geometry of Methyl Orange

Bond Angles, deg

C^{sp^2}-C^{sp^2}-C^{sp^2}	120.0	C^{sp^2}-N-N	120.0
C^{sp^2}-S-O	109.5	C^{sp^2}-N-C^{sp^2}	109.5
C^{sp^2}-C^{sp^2}-H	120.0	N-C^{sp^2}-H	109.5
O-S-O	109.5	H-C^{sp^3}-H	109.5
C^{sp^2}-C^{sp^2}-N	120.0		

Bond Lengths, Å

C^{sp^2}-S	1.50	C^{sp^2}-N	1.34
S-O	1.57	N-N	1.30
C^{sp^2}-C^{sp^2}	1.40	C^{sp^3}-H	1.09
C^{sp^2}-H	1.08	N-C^{sp^3}	1.47

Intermolecular modeling has been carried out by first selecting "reasonable" diverse starting structures, based upon computer graphics visualization, and then allowing the mobile molecule to find an intermolecular potential energy minimum. This procedure does not guarantee that the global energy minimum will be identified, because the number of polymer–dye complex states sampled is limited. The intermolecular energy minima located via this process may, however, give feedback information as to other starting structures that should be sampled.

Valence Geometries. A. Methyl Orange. The bond lengths and angles for methyl orange are listed in Table I. The partial atomic charges, calculated by the MNDO[5] approximation, are listed in Table II. The atom numbering scheme of the dye is shown in Figure 2.

B. Poly(*N*-vinylimidazoles). The valence geometry of PVI is given in Table III. The geometry of the imidazole ring has been obtained by complete MNDO[5] geometric optimization using the experimentally determined crystal structure as the starting point.[6] The experimental structure could not be used directly because intermolecular hydrogen bonding within the crystal structure produces valence geometry distortions. Both isotactic and syndiotactic structures have been considered. Only the isotactic

Table II
MNDO Partial Charges for Methyl Orange

atom number	atom letter	partial charge	atom number	atom letter	partial charge
1	C	−0.71	18	C	0.01
2	C	0.05	19	C	−0.05
3	H	0.08	20	H	0.09
4	C	−0.06	21	C	−0.04
5	H	0.05	22	H	0.07
6	C	−0.03	23	N	−0.30
7	N	−0.08	24	C	0.15
8	C	−0.07	15	H	0.01
9	H	0.06	26	H	−0.03
10	C	0.05	27	H	−0.00
11	H	0.07	28	C	0.15
12	N	−0.15	29	H	−0.00
13	C	0.01	30	H	−0.03
14	C	−0.12	31	H	0.01
15	H	0.06	32	S	2.73
16	C	−0.00	33	O	−1.01
17	H	0.07	34	O	−1.01
			35	O	−1.01

Table III
Valence Geometry of PVI

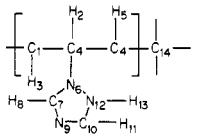

Bond Angles, deg

1-4-6	109.5	6-7-8	123.4
1-4-14	114.0	6-7-9	110.2
2-1-3	109.5	6-12-10	104.9
2-1-4	108.0	7-9-10	106.0
4-1-3	108.0	8-7-9	126.0
4-6-7	120.0	9-10-11	120.8
4-6-12	120.0	9-10-12	110.6
5-4-1	108.0	10-12-13	123.4
5-4-6	109.5	11-10-12	128.6
5-4-14	108.0	12-6-7	108.3
		13-12-6	121.7

Bond Lengths, Å

1-4	1.54	7-9	1.34
1-2	1.09	9-10	1.39
4-6	1.43	10-11	1.09
6-7	1.39	10-12	1.39
6-12	1.41	12-13	1.09
7-8	1.09		

results are reported, since they alone correspond favorably to the experimental observations.[1]

Partial atomic charges for PVI have been determined from MNDO[5] calculations performed on a pentamer. These charges are reported in Table IV. The charge density on N9 (−0.19) is less negative than that of N6 (−0.26). This is a surprising finding and may be an artifact of MNDO. However, the difference in charges is sufficiently small so as to have a very minor effect on the overall relative energetics.

The charge distribution located on the central monomer has been selected as the model for an infinite chain. The charges for the imidazole ring and the polymer backbone have been assumed to be the same for the benzyl-substituted PVI as for unsubstituted PVI. In turn, the charges for the methylene and phenyl groups were restricted to be identical with those found on methyl-substituted benzene. The total molecular charge for a monomer of a substituted PVI is $-n$. The negative charge per monomer has been localized at the substituted imidazole nitrogen. The substituted-nitrogen charge has been determined by subtracting a value of 1 from the charge found on the PVI unsubstituted nitrogen. This charge–structure fragment approach has been described in detail.[7]

Table IV
MNDO-Calculated Partial Charges for PVI[a]

atom number	atom letter	partial charge
1	C	−0.04
2	H	0.01
3	H	0.01
4	C	0.15
5	H	0.04
6	N	−0.26
7	C	0.05
8	H	0.12
9[b]	N[b]	−0.19[b]
10	C	−0.04
11	H	0.11
12	C	−0.07
13	H	0.10

[a] See Table III for numbering. [b] N^+ has partial charge of 0.81.

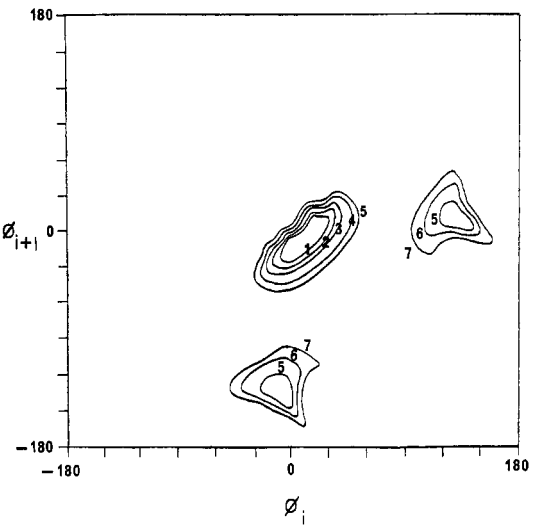

Figure 3. Conformational energy map for the adjacent backbone rotations ϕ_i and ϕ_{i+1} for PVI. The energy contours are in kcal/mol above the global energy minimum. $\phi_i = \phi_{i+1} = 0$ corresponds to the all-trans planar backbone conformation.

Results

Intramolecular Conformational Analyses. A. PVI. The potential energy surface is similar to that found for isotactic polystyrene.[4,8] The global energy minimum corresponds to a nearly all-trans conformation. Only slight perturbations along the polymer backbone are necessary to relieve the strain between adjacent imidazole rings. Studies of isotactic polystyrene[4,8-10] show that the energetic feasibility of the near-all-trans conformation is highly dependent upon the choice of steric potentials and/or valence geometry. The Hopfinger potential set[2] is relatively soft with regard to the aromatic carbon atom. However, the softness of this potential set does not prevent identification of all energy minima. Difficulties arise only when an estimate of the relative stabilities of various stable conformers is attempted.

The calculations for the PVI polymer suggest the 3/1 helical form to be more than 5 kcal/mol/monomer less stable than the extended helical forms (the softness of the potential function favors the near-all-trans conformations). It is apparent from Figure 3 that the near-all-trans (ϕ_i = 10° and ϕ_{i+1} = 20°) and 3/1 [(ϕ_i, ϕ_{i+1}) = (0°, −120°) or (120°, 0°)] helical forms correspond to the low-energy regions. The 4/1, 5/1 ... helices lie close to the 3/1 helix on the (ϕ_i, ϕ_{i+1}) surface and are also low-energy structures.

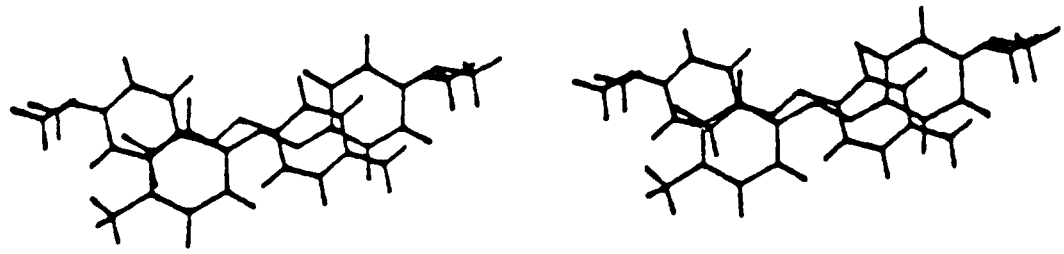

Figure 4. Global energy minimum of a dye–dye complex.

That is, small changes in ϕ_i and ϕ_{i+1} from a 3/1 helix generate higher order helices.

B. Poly(3-methyl-1-vinylimidazolium bromide) (MPVI). The conformational energy map of methyl-substituted PVI is quite similar to that of the unsubstituted polymer. Isotactic poly(*p*-fluorostyrene)[11] is believed to crystallize with the polymer chain in a 4/1 helix. The methyl group in MPVI has an effect similar to that of the fluorine atom and may also promote formation of a 4/1 helix in the crystal. The stronger force center on the ring enhances the stabilities of the less extended helical forms (i.e., the 3/1 and 4/1 helices). Thus although the near-all-trans conformation is still favored, the 3/1 helix is now within 3 kcal/mol of the global minimum, in contrast to the 5 kcal/mol for PVI. Again, the softness of the aromatic potential favors the near-all-trans conformation.

C. Poly(3-benzyl-1-vinylimidazolium bromide) (BPVI). Two additional degrees of rotational freedom exist for the benzyl-substituted PVI: rotations about the imidazole nitrogen–methylene carbon and the methylene carbon–phenyl carbon bonds. These two bond rotations have been allowed with the polymer backbone fixed in either a 12/1 or 3/1 helix. The 12/1 helix has been selected as a model for the near-all-trans minimum-energy conformer state. The plane of the imidazole ring has been fixed in a position perpendicular to the polymer backbone. An analysis of the energy maps shows that more side-chain rotational freedom is available when the polymer backbone is in a 3/1 helix. The greater distance between adjacent imidazole rings is consistent with this finding. The global energy minima for the 3/1 and 12/1 helices are at ϕ(I-(N)–CH_2–) = 90° and −80° and ϕ(–CH_2–C_6H_5) = −40° and 150°, respectively. The energy minimum for the 12/1 helix is at an unrealistically high value of about 60 kcal/mol/monomer! This demonstrates that steric hindrance between adjacent rings prevents the benzyl-substituted PVI from adopting a 12/1 helix and, more generally, any of the near-all-trans conformations.

D. Methyl Orange. The intramolecular energy was first considered as the sum of steric, hydrogen-bonding, and electrostatic interactions, excluding intrinsic torsional terms. The two nitrogen–phenyl carbon bonds were allowed to rotate between −180° and 170° in 10° increments. The dye is quite flexible, and hindrance to bond rotation, if any, will be due to the missing torsional component. However, the MNDO[5]-derived intrinsic torsional potential for the two identical bonds can be represented as $P(\phi) = 0.76 \sin^2 \phi^2$. This torsional barrier is small, and it is concluded that the methyl orange is, overall, quite flexible in conformation relative to the polymers.

Intermolecular Interactions. A. Dye–Dye Interactions. Two dye molecules have been allowed to interact. Each molecule has been restricted to a trans configuration with the phenyl rings coplanar. The choice of coplanarity represents a practical geometric constraint based upon the general observation that multiring molecules crystallize in a coplanar arrangement. Fifty uniformly distributed (over intermolecular space) starting points have been selected and the intermolecular energy has been minimized.

The various local intermolecular energy minima have an expected common feature—the highly charged sulfonate groups are as far apart as possible, whereas the dye molecules maintain a maximum amount of intermolecular phenyl-ring overlap. Figure 4 shows a stereoview of the lowest energy binary complex (∼−33 kcal/mol/binary complex). All other local energy minima complexes within 10 kcal/mol/binary complex of the lowest energy complex differ only in the extent of phenyl-ring overlap.

B. Polymer–Dye Interactions. A single molecule of methyl orange has first been allowed to interact with a segment of a polymer chain under the fixed conformational constraint. A chain segment of 13 monomer units has been used to model the polymer. This allows the possibility that the dye molecule might lie parallel to the polymer chain axis. Thus, both phenyl rings of the dye molecule would be able to interact with two imidazole rings of the polymer.

PVI and BPVI have been restricted to a 3/1 helical conformation. However, MPVI has been considered as both a 3/1 and 4/1 helix.

The near-all-trans conformations have been excluded from the polymer–dye calculations because they eliminate the possibility for the dye molecule to intercalate between the spatially close imidazole rings of the polymer. The only type of polymer–dye complex that might occur when the near-all-trans structures are used would result totally from electrostatic interactions between the sulfonate group of the dye and the charged imidazole nitrogen of the polymer side chain. This type of interaction is also possible in the other stable helical forms (3/1, 4/1, etc.). However, experimental findings[1] indicate that the dye–polymer interactions involve both van der Waals and electrostatic interactions. Thus it is reasonable to delete complex modes governed solely by electrostatic behavior and, consequently, the near-all-trans polymer chain conformations.

The intermolecular polymer–dye energy minimizations have been carried out with 8 to 10 different starting structures for each polymer and its particular conformation (3/1 or 4/1 [MPVI] helix). The starting points were selected to correspond to binding modes that promote either intercalation of the dye between imidazole rings or direct interactions between charge centers. For each of these two general types of binding the relative orientation of the dye was varied with respect to the central monomers of the polymer segment. Clearly, this procedure does not completely sample intermolecular space, and minima can be missed. However, the repetitious convergence to the same final structure from different starting points suggests this approach is adequate.

The introduction of variation of the "molecular dielectric constant" has been superimposed on the multiple starting points in the energy minimizations. The dielectric was assigned values of 3.5, 7.0, 30, and 60. Principal attention has been given to the results obtained for $\epsilon = 30$, since this

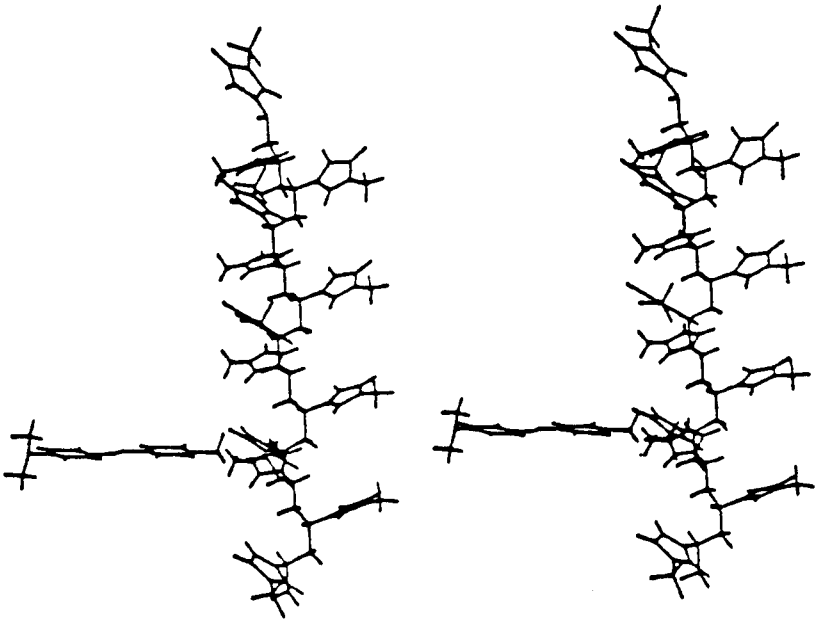

Figure 5. Global energy minimum of a MPVI–dye complex for $\epsilon = 3.5$.

value is suggested from the experimental studies.[1] The reason for varying ϵ has been to gain an understanding as to how this ill-defined factor affects the results of the structural calculations. In essence, ϵ has been treated as a scaling factor.

i. MPVI–Dye (3/1 Helix). The general orientation of the dye molecule relative to the polymer segment is dependent upon the value for ϵ. The binding trends are not significantly altered when ϵ is changed from 3.5 to 7.0. The steric energy component increases and the electrostatic component decreases by ~50% when ϵ is raised from 3.5 to 7.0, but the electrostatic energy remains 4 times the magnitude of the steric energy. The orientations of MO to the polymer for the global minima for $\epsilon = 3.5$ and 7.0 has the dye, in each case, close to the substituted imidazole nitrogen of the polymer. That is, the binding is governed primarily by electrostatic interactions, which is at odds with experimental data.[1] The global energy minimum binary complex is shown in Figure 5 for $\epsilon = 3.5$.

The most stable polymer–dye complexes for $\epsilon = 30$ and 60 are virtually identical and characterized by the intercalation (insertion) of the dye between adjacent overlapping imidazole rings. Intercalation takes place at the expense of the ionic interaction between the sulfonate of the dye and the nitrogens of the overlapping imidazole rings. The global energy minimum complex for $\epsilon = 30$ is shown in Figure 6.

ii. MPVI–Dye (4/1 Helix). Electrostatic interactions again dominate the dispersive–steric interactions when the dielectric is either 3.5 or 7.0. Surprisingly, however, the twist of the 4/1 helix increases the distance between *adjacent overlapping* imidazole rings (relative to the 3/1 helix), but decreases the distance between rings of *adjacent monomer units*, so that the phenyl ring of the dye and the imidazole rings of the polymer cannot strongly overlap/interact, owing to steric constraints. Even when ϵ is assigned a value of 60, the energy due to steric interactions is only half that resulting from electrostatic interactions. Thus all stable binding complexes for the 4/1 helix of MPVI are controlled by electrostatic interactions. Consequently, it is reasonable to dismiss the 4/1 helix as the "binding conformation" for the polymer since electrostatic interaction is not the dominant driving force for binding.[1]

iii. BPVI–Dye (3/1 Helix). The geometric and energetic behavior of BPVI interacting with the dye is quite similar to that of the MPVI–dye complexes. The phenyl groups of BPVI are oriented such that the sulfonate group of the dye may still bind directly to the substituted nitrogen at low dielectric values (3.5 and 7.0). At high values of ϵ (30 and 60), the dye intercalates between pairs of adjacent overlapping side chains. However, the intercalation is characterized by the direct overlap of the polymer phenyl rings and a dye phenyl ring. This is in contrast to PVI–dye and MPVI–dye complexes, in which intercalation involves the polymer imidazole rings with a phenyl from methyl orange. The BPVI–dye complex is shown in Figure 7.

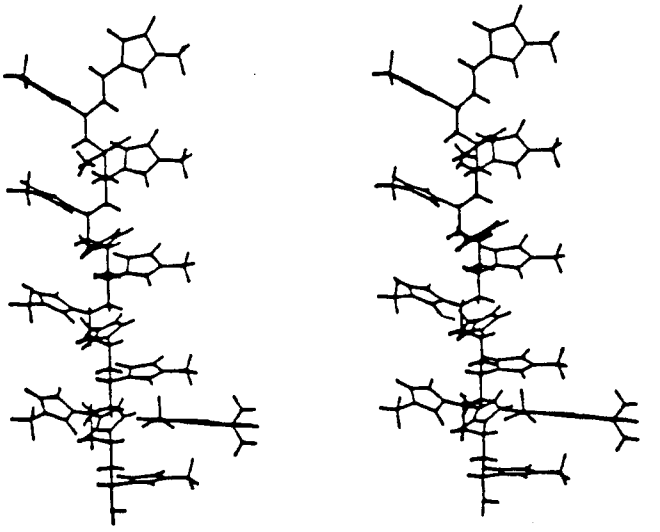

Figure 6. Global energy minimum of a MPVI–dye complex for $\epsilon = 30$.

iv. PVI–Dye (3/1 Helix) and Intermolecular Energetics Analysis. Limited intermolecular energy studies involving PVI and the dye have been carried out for completeness. The dye was initially placed at the energy minimum found for the MPVI–dye complex in which $\epsilon = 30$. The intermolecular energy of the PVI–dye complex was subsequently minimized for $\epsilon = 30$ only. The dye moves very little from its starting position, and the resulting PVI–dye complex is nearly identical with that shown in Figure 6 for MPVI–dye. However, the strength of binding is diminished, owing to a loss in the electrostatic

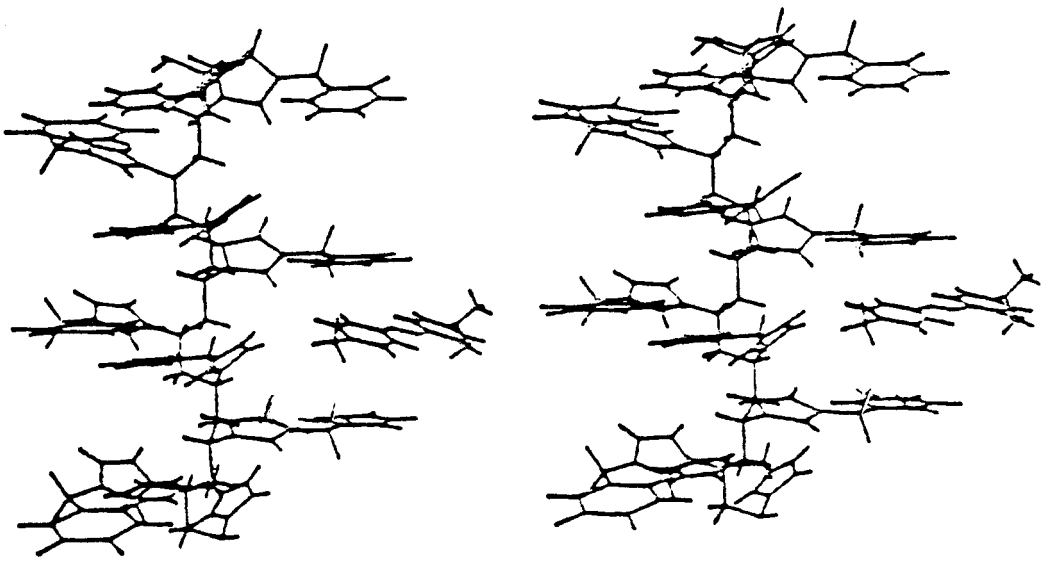

Figure 7. Global energy minimum of a BPVI–dye complex for $\epsilon = 30$.

Table V

A. Intermolecular Polymer-Dye Complexing Energies (E_0) in kcal/mol/Binary Complex for $\epsilon = 30$[a]

complex	steric-dispersive	electrostatic	total
PVI-dye	−14.96	−22.44	−36.40
MPVI-dye	−15.31	−20.35	−35.66
BPVI-dye	−20.05	−16.65	−36.70

B. Experimental ΔH of Binding in kcal/mol at Low Binding Concentrations ($r = 0.01$)

polymer	ΔH
PVI	−4.4
MPVI	−3.1
BPVI	−6.0

[a] A single dye is interacted with the polymer chain segment in a 3/1 helical conformation.

attraction upon side-chain charge neutralization.

The set of calculated intermolecular energies for each of the three polymer–dye complexes and the dye–dye dimer are reported in Table V. The experimental binding enthalpies for the low-saturation region ($r = 0.01$) are also reported in Table V.

The absolute values of the calculated energies have little physical meaning. However, relative energies (energy differences) between pairs of complexes are thermodynamically meaningful. It can be seen from Table V that theory and experiment agree in the ranking of interaction energies:

$$\text{BPVI–dye} > \text{PVI–dye} > \text{MPVI–dye} \qquad (2)$$

Moreover, the energy differences between computed binding energies of pairs of complexes are quite similar to the measured values. This agreement may be fortuitous since many interactions at play in the real system are neglected in the calculations.

The total polymer–dye binding energy differences for the three polymers are small. However, the corresponding individual steric and electrostatic component energy differences are much larger, suggesting the computed relative energetics are meaningful and significant. Moreover, the polymer–dye binding energies are each larger than the dye–dye binding energy. This suggests that the modeling energetics predicts polymer binding as a favorable thermodynamic process over dye dimerization. Again this may be something of an artificial result, since dye–solvent and polymer–solvent interactions are lumped into the dielectric factor (by presumably setting $\epsilon = 30$) along with other contributions.

Nevertheless, if the results of the calculations are accepted as meaningful, it is possible to interpret the experimental binding observations in terms of competing steric–dispersive and electrostatic interactions. In essence, the addition of CH_3 and $-CH_2C_6H_5$ to PVI at the nitrogen imidazole enhances the steric–dispersive binding interactions at the expense of favorable electrostatic energetics. The CH_3 and $-CH_2C_6H_5$ sterically prevent the sulfonate group of the dye from being as close to the charged ring nitrogen as in PVI. However, the additional force centers increase dispersive energetics. In aqueous solution hydrophobic effects (entropic gain due to hydration changes upon interaction) may contribute to the thermodynamics, but these have not been addressed in these calculations.

C. Multiple Dye–(MPVI–Dye) Interactions. The final series of calculations carried out on the polymer–dye system has been to consider multiple dye binding to MPVI in a 3/1 helix for $\epsilon = 30$. A dye was placed between the imidazole rings of monomers i and $i + 3$ in its minimum-energy intercalation state shown in Figure 6. A second dye was placed at various sites involving rings $i + j$ and $i + j + 3$, where $j = 1$–6. The second dye was also inserted in the minimum-energy intercalation state illustrated in Figure 6. Figure 8 shows the resultant binary dye–MPVI complex for $j = 3$. In doing this it has been assumed that all dye–MPVI binding geometries, irrespective of their distribution of locations along the polymer chain, are identical. This simplification makes it possible to compute the total binding energy E_b of any distribution of N dye-site binding modes by only knowing the distribution scheme

$$E_b = NE_0 + \sum_{k=0}^{j-1} m_k E_k \qquad (3)$$

E_0 is the dye–polymer binding energy reported in Table V, and m_k is the number of dye–dye interactions separated by k imidazole rings along the chain. E_k are the corresponding dye–dye interaction energies, which have been computed by using the geometries described above and are reported in Table VI.

The application of the values of E_k in Table VI to eq 3 suggests that binding strength should increase as dye binding increases, since all the E_k are negative. This is in agreement with experimental results. Second, the values

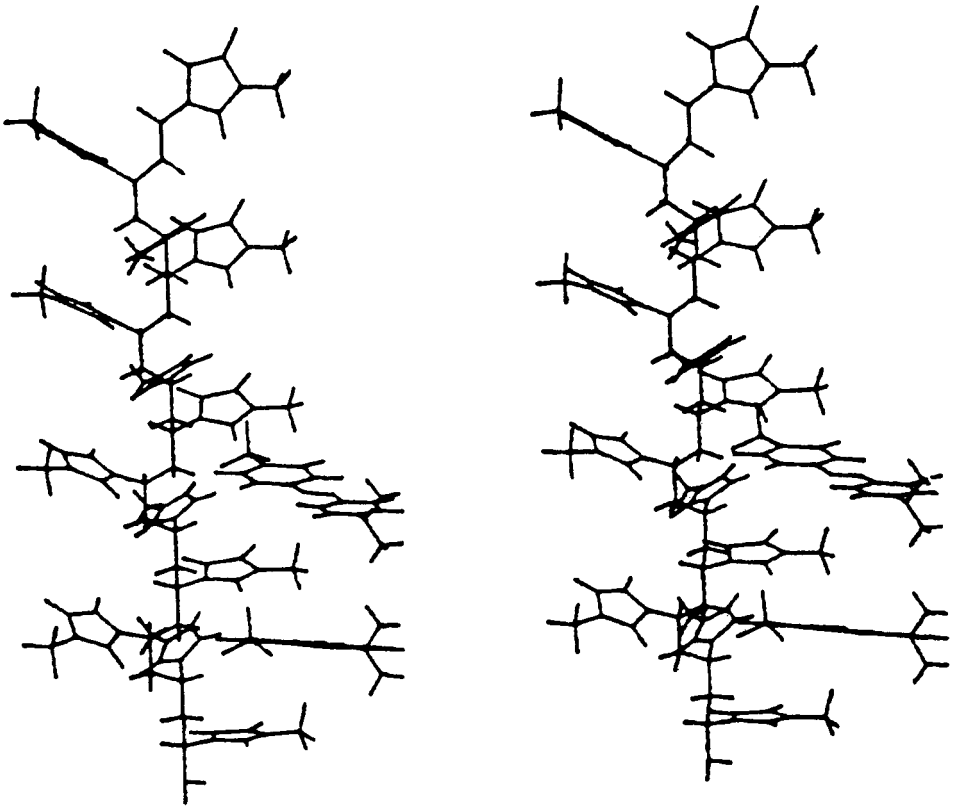

Figure 8. Global energy minimum of a MPVI-$(dye)_2$ complex for $j = 3$ and $\epsilon = 30$.

Table VI
Energetics of Bound Dye-Bound Dye Interactions Using the Minimum Energy MPVI-Dye Geometry for Each Binding Site

k[a]	dispersive-repulsive steric energy, kcal/mol	electrostatic energy, kcal/mol	total energy (E_k), kcal/mol
0	-7.85	-6.10	-13.95
1	-5.08	-7.25	-12.33
2	-6.03	-2.03	-8.06
3	-4.09	-5.33	-9.42
4	-2.49	-3.86	-6.35
5	-1.42	-1.94	-3.36

[a] Number of imidazole rings separating pairs of ring-dye-ring intercalation complexes.

for E_k in Table VI suggest cooperative binding should take place up through $k = 1$, that is "second-nearest-neighbor" interactions. However, for $k = 2$ the E_k becomes more positive (less stabilizing) than for $k = 3$. This suggests that the cooperative mode of binding would favor formation of adjacent triplets of dye molecules separated by an empty binding site. Another way of stating this is that cooperative binding should occur until 75% (3 of 4 sites) are occupied. Cooperativity is predicted to be diminished or lost above 75% occupancy, which is consistent with experimental findings.[1]

Discussion

Three assumptions have been made in this molecular modeling study: (1) The local conformation of the polymer adopted in the polymer–dye complex is a perturbation of one of the stable isolated-chain conformers. (2) Stable all-isotactic or all-syndiotactic chain conformations may be used to model short-range atactic chain segments involved at low dye-binding concentrations. (3) Contributions to the electrostatic potential energy from the ionic aqueous medium, dye, and polymer can be effectively represented by setting the dielectric constant in a Coulomb potential equal to 30 for both intra- and intermolecular interactions.

The "molecular dielectric" term is critical to specifying the molecular energetics and geometry in charged systems such as those studied here. Unfortunately, no satisfactory approach to meaningfully treating the molecular dielectric has emerged. There have been some attempts to characterize the spatial variability of ϵ in coulombic functions for uncharged systems.[2,12] Functional forms have also been proposed for the dielectric behavior in simple ionic crystals[13] but do not appear to be easily translated into a molecular-mechanics force field. Thus, there is currently an impasse in treating molecular dielectric contributions to electrostatic interactions. Fortunately, in the computational investigations reported in this paper it has been possible to assign a value (30) to ϵ in a simple coulomb potential on the basis of experimental data. The reliability of the computational findings presented here depends upon the accuracy of this dielectric value assignment. Still, it must be kept in mind that setting $\epsilon = 30$ is a crude attempt to take into account several type of interactions which include the following: (1) polymer–aqueous solvent and dye–aqueous solvent hydration interactions, (2) solvent–solvent interactions for the aqueous medium, and (3) dielectric disperisivity of polymer–dye and dye–dye electrostatic interactions due to the aqueous media and the organic nature of the polymer and dye in themselves.

Counterions were not considered in the calculations because of additional complications involving the dielectric factor and also because of inadequate potential functions to describe their interactions with organic species. Thus the computational findings of this work apply only to polymer–dye–aqueous systems at very high, or total, counterion dilution.

Our proposed binding model must fail at high dye-binding concentrations since an all-isotactic chain segment

has been used to describe the local dye-binding geometry of an atactic polymer. The model predicts preferential dye binding to isotactic chain segments which, when used up at high dye-binding concentrations, leaves only nonisotactic chain segments available. Both the geometry and energetics involved at these nonisotactic binding sites will be different from the isotactic model.

The reasonableness of the polymer–dye binding geometries determined from the computations reported here rests upon the following agreements between the calculations and experimental observations: (1) The polymer–dye binding constant increases as the extent of binding increases. (2) The interaction energy between the dye and the polymer decreases in the order BPVI–dye > PVI–dye > MPVI–dye. (3) Electrostatic and dispersive–repulsive (van der Waals) interactions jointly control polymer–dye binding. The model predicts that this combination control of dye binding is a result of the dye intercalating between spatially adjacent side-chain rings in the polymer. (4) There is cooperative dye binding until about 70–80% of the binding sites are occupied. At higher bound-site concentrations the cooperativity cannot persist. (5) The computed and observed relative differences in binding energy of the dye to PVI, MPVI, and BPVI are, correspondingly, nearly identical. The consistency between theory and experiment described above is contingent upon (a) $\epsilon = 30$, (b) local isotactic chain segment tacticity, and (c) a 3/1 helical conformation.

Other experimental observations and conclusions mentioned in the Introduction could not be addressed in the computations because of two limitations: the effective dielectric of the uncharged system was not available from experimental information, and explicit contributions from counterion and water molecules could not be modeled.

Nevertheless, there is sufficient agreement between theory and experiment to suggest that the predicted charged polymer–dye binding modes, and corresponding molecular geometries, should be considered as working models for conceptualizing molecular behavior in future studies.

Acknowledgment. B. J. Orchard and A. J. Hopfinger thank Eastman-Kodak Company for the financial support for this study. We also appreciate the helpful discussions and suggestions of R. A. Pearlstein and D. Malhotra of Case Western Reserve University during this study.

Registry No. PVI, 25232-42-2; MPVI, 87323-11-3; BPVI, 88337-18-2; methyl orange, 547-58-0.

References and Notes

(1) Tan, J. S.; Handel, T. M. *Polym. Prepr., Am. Chem. Soc., Div. Polym. Chem.* **1982**, *23*, 48 and unpublished work.
(2) Hopfinger, A. J. "Conformational Properties of Macromolecules"; Academic Press: New York, 1973.
(3) (a) Pearlstein, R. A.; Malhotra, D.; Harr, R.; Orchard, B. J.; Tripathy, S. K.; Hopfinger, A. J.; Potenzone, R., Jr. "A New Molecular Modeling Software System: The Chemical Modeling Laboratory (CHEMLAB). I. Overview of the System. II. Three-Dimensional Structure Modeling" (in preparation). (b) Pearlstein, R. A. "CHEMLAB Users Guide", available through Molecular Design Ltd., Hayward, CA 94541.
(4) Orchard, B. J.; Tripathy, S. K.; Pearlstein, R. A.; Hopfinger, A. J.; Taylor, P. L. *Macromolecules*, submitted for publication.
(5) Dewar, M. J. S.; Thiel, W. *J. Am. Chem. Soc.* **1977**, *99*, 4899.
(6) Martinez-Carrera, C. *Acta Crystallogr.* **1966**, *20*, 783.
(7) Potenzone, R. Ph.D. Thesis, Department of Macromolecular Science, Case Western Reserve University, Cleveland, OH, 1978.
(8) Yoon, D. Y.; Sundararajan, P. R.; Flory, P. J. *Macromolecules* **1975**, *8*, 776.
(9) Atkins, E. D. T.; Isaac, D. H.; Keller, A. J. *J. Polym. Sci., Polym. Phys. Ed.* **1980**, *18*, 71.
(10) Sundararajan, P. R.; Tyrer, N. J.; Bluhm, T. L. *Macromolecules* **1982**, *15*, 286.
(11) Farmer, B. L.; Lando, J. B. *J. Macromol. Sci., Phys.* **1974**, *B10*, 381.
(12) Hopfinger, A. J. In "Peptides, Polypeptides and Proteins"; Blout, E. R., Bovey, F. A., Goodman, M., Lotan, N., Eds.; Wiley: New York, 1974; p 71.
(13) Tripathy, S. K.; Hopfinger, A. J.; Taylor, P. L. *J. Phys. Chem.* **1981**, *85*, 1371.